Biosensors and Bioelectronics 57 (2014) 226–231

Contents lists available at ScienceDirect

Biosensors and Bioelectronics

journal homepage: www.elsevier.com/locate/bios

A fluorescent aptasensor based on DNA-scaffolded silver-nanocluster for ochratoxin A detection

Jinghua Chen [a], Xi Zhang [a], Shuxian Cai [a], Dongzhi Wu [a], Mei Chen [a], Shihua Wang [b,*], Jing Zhang [b,*]

[a] Department of Pharmaceutical Analysis, Faculty of Pharmacy, Fujian Medical University, Fuzhou 350108, Fujian, China
[b] The Ministry of Education Key Laboratory of Biopesticide and Chemical Biology, and College of Life Sciences, Fujian Agriculture and Forestry University, Fuzhou 350002, Fujian, China

ARTICLE INFO

Article history:
Received 28 September 2013
Received in revised form
2 February 2014
Accepted 5 February 2014
Available online 12 February 2014

Keywords:
Fluorescent aptasensor
OTA
DNA-scaffolded silver-nanocluster
Structure-switching
Magnetic beads

ABSTRACT

The selective detection of ultratrace amounts of ochratoxin A (OTA) is extremely important for food safety since it is one of the most toxic and widespread mycotoxin. Here we develop a signal-on fluorescent biosensor for detection of OTA based on fluorescent DNA-scaffolded silver-nanocluster (AgNCs), structure-switching of anti-OTA aptamer (Ap) and magnetic beads (MBs), and demonstrate its feasibility in the application of detecting OTA in real samples of wheat. The method exhibits superior sensitivity with a detection limit as low as 2 pg/mL OTA with high specificity. To the best of our knowledge, this is the first attempt to detect OTA based on DNA-scaffolded AgNCs, which possesses relatively high fluorescence quantum yield and photostability with regard to traditional organic dyes and quantum dots. Moreover, combined with the merits of MBs and aptamer, the proposed sensor has many advantages such as fabrication easiness, operation convenience, low cost, and being fast and portable, which may represent a promising path toward routine OTA control.

1. Introduction

With the growing awareness of healthy diet, food safety has become a hot button across society. Foodborne intoxications are one of the most enduring risks for public health and have been increasing worldwide concern. Especially, OTA is the most toxic mycotoxin with the nephrotoxic, immunotoxic, teratogenic and carcinogenic effects (Clarke et al., 1993). The International Agency for Research on Cancer (IARC) has classified OTA in 2B Group (possibly carcinogenic agent) (O'Brien and Dietrich, 2005). What makes it worse is that OTA is the most widespread naturally occurring mycotoxin and exists in many food products throughout the world including cereals, wheat, corns, oats, coffee beans, beer, coffee, grape juice and wine. Therefore, it is of great significance to develop a sensitive, cheap, fast and simple method for large scale OTA detection performed by grain handlers and agricultural product manufacturers themselves.

Very recently, there has been a tremendous increase in reports on many aptamer-based biosensors (aptasensors) for OTA detection (Yang et al., 2011; Sheng et al., 2011; Chen et al., 2012). Compared with the currently accepted testing methods, such as high performance liquid chromatography (HPLC) coupled to mass spectrometry (MS) or tandem mass spectrometry (MS/MS) and enzyme-linked immunosorbent assays (ELISA), aptasensors have many significant advantages including higher sensitivity and selectivity, fabrication easiness, operation convenience and speed (Tong et al., 2012). In particular, many fluorescent aptasensors for OTA detection have been developed. Cruz-Aguado and Penner first applied the OTA aptamer for the detection of OTA with fluorescence polarization assays (Cruz-Aguado and Penner, 2008a, 2008b). However, the method required multiple, complex and time consuming steps that definitely hampered further application for rapid field detection of OTA. Chen et al. developed a fast and reliable fluorescent sensing platform for OTA detection based on a target-induced structure-switching signaling aptamer (Chen et al., 2012). Nevertheless, the method required modifications of fluorescein and quencher moiety, which made it complicated and expensive. Furthermore, the sensitivity of the method was not high enough for the OTA detection in real samples.

It is worth noting that DNA-scaffolded AgNCs using DNA as a template have attracted a great deal of attention as novel fluorophores for DNA biosensing (Guo et al., 2010; Huang et al., 2011; Ma et al., 2011). Compared with the most commonly used signal transducers including organic dyes, quantum dots, and redox reporters, which are of high cost, poor photostability and biocompatibility or toxic, DNA-scaffolded AgNCs have an appealing set of features such as outstanding photostability, high quantum yield, nontoxicity,

* Corresponding authors. Tel./fax: +86 591 83769155.
E-mail addresses: wshyyl@sina.com.cn (S. Wang), 1601225385@qq.com (J. Zhang).

http://dx.doi.org/10.1016/j.bios.2014.02.001
0956-5663

biocompatibility and facile synthesis (Diez and Ras, 2011). Moreover the fluorescence emission of AgNCs can be fine-tuned throughout the visible and near-IR range simply by modulating the sequence and length of used DNA (Richards et al., 2008). In addition, E.G. Gwinn et al. found, compared with a hairpin or a loop, that linear oligonucleotides mainly consisting of 12 bases were excellent scaffolds for the formation of emissive AgNCs by sodium borohydride ($NaBH_4$) reduction of solutions with molar ratio bases:Ag 2:1 (Richards et al., 2009). Furthermore, cytosine bases have a higher affinity for silver compared to other bases, and AgNCs templated in linear 12-mer cytosine oligonucleotide produce four emitters with fluorescence quantum yield up to 17% (Ritchie et al., 2007). Many recently reported that AgNC-based methods have been successfully applied in cellular labeling or imaging, detecting various targets including miRNA, ssDNA and metal ion (Huang et al., 2011; Yang and Vosch, 2011; Lan et al., 2010). Lan et al. (2010) developed a novel method to quantify attomolar miRNA by DNA-scaffolded AgNCs probe based on isothermal amplification (Liu et al., 2012). Yin et al. developed a one-step strategy for target tumor cell recognition and analysis based on fluorescent AgNCs–aptamer assemblies (Yin et al., 2012). However, the method for OTA detection based on AgNCs has never been reported up to now. If AgNCs can be used in fluorescent aptasensors for OTA detection, the sensitivity and reproducibility of the method will be improved greatly due to the high quantum yield and photostability of AgNCs. At the same time, the pollution to the environment of the assay will be decreased dramatically owing to the nontoxicity of AgNCs.

Nowadays, as a versatile tool for various biosensors, MBs have received considerable attention. On one hand, they can be used as a carrier for reagent or analyte pre-concentration. On the other hand, MBs modified with different recognition elements have been used for specific capture of different molecules. Due to the fact that MBs can be finely manipulated in a complicated system with a magnetic field, MBs-based methods possess higher sensitivity and analytical speed and are easier to be integrated with diverse assay processes in a high performance test.

Stimulated by the above studies, an ultra-highly sensitive and selective, signal-on fluorescent aptasensor based on the AgNCs, structure-switching of anti-OTA aptamer and MBs was developed here for detection of OTA in wheat. Using this strategy, it was possible to detect OTA through a linear dynamic range of 0.01–0.3 ng/mL with a detection limit down to 2 pg/mL. In comparison with former methods, such as “target-induced strand release coupling cleavage of nicking endonuclease” and “aptasensor based on real-time quantitative PCR”, which need complicated labeling and multiple procedures, enzyme-aided reaction or precise control of the experimental temperature, the method we herein reported has obvious advantages such as enzyme-free, operation convenience, short detection time, low cost and so on (Hun et al., 2013; Ma et al., 2013). Furthermore, because the photoluminescence emission band of DNA–AgNCs can be fine-tuned just by changing the sequence and length of used DNA, we envision that the proposed aptasensor holds great potential to be used in combined and simultaneous detection of multiple mycotoxins. Because many agricultural products are often contaminated by many kinds of mycotoxins during their growth, harvest, storage and shipment, the proposed aptasensor may represent a promising path toward routine quality control of food safety.

2. Experimental section

2.1. Reagents and apparatus

All oligonucleotides were synthesized by Sangong Biotech (Shanghai, China) Co., Ltd. and their base sequences were illustrated in *Table S1 (see details* from the support information). The concentrations were quantified by OD260 based on their individual absorption coefficients. Streptavidin-modified magnetic beads (10 mg mL^{-1}) were purchased from Dynal Biotech ASA (Oslo, Norway). OTA, ochratoxin B (OTB), aflatoxin B1 (AFB1) and fumonisin (FB) were purchased from Sigma-Aldrich (Shanghai, China). Silver nitrate, sodium borohydride and trisodium citrate were purchased from Sinopharm Chemical Reagent Company (Shanghai, China). Tris-(hydroxymethyl) aminomethane(Tris) was purchased from Cxbio Biotechnology Co. Ltd. (Denmark). DNA immobilization and hybridization buffer were all the mixture of 10 mM Tris, 1.0 mM EDTA, 0.01% Tween 20 and 1 M $NaNO_3$(pH 7.5). The sodium citrate buffer (10 mM, pH 7.0) was used as binding buffer for the synthesis of AgNCs. All solutions were prepared with MilliQ water (18.2 MΩ) and all other chemicals were of analytical grade.

The fluorescence spectra were recorded with a Cary Eclipse fluorescence spectrometer (Agilent Technologies). UV/vis absorbance spectra were measured with a UV-2450 spectrophotometer (SHIMADZU, Japan) using a quartz cell with 1.0 cm optical pathway. The circular dichroism (CD) spectra were studied based on the Jasco J-810 circular dichroismspectropolarimeter (Tokyo, Japan). High response transmission electron microscopy (HRTEM) was *performed by* a JEM-2010 microscope (JEOL Ltd., Japan).

2.2. Ap self-assembly and hybridization at the magnetic beads

The stock solutions of all the DNAs were preheated to 88 °C for 5 min and incubated at room temperature for at least 30 min before use. Ap self-assembly was carried out using a procedure based on that recommended by Dynal Biotech ASA (Oslo, Norway). A volume of 50 μL of streptavidin coated MBs was poured into a 2.0 mL centrifuge vial. Under the magnetic field, the microspheres were washed three times with immobilization buffer and resuspended in 125 μL of the same buffer containing 2.5 μmol of biotinylated Ap. Then the Ap was captured onto the MBs during 30 min at 37 °C with gentle mixing. Subsequently, the Ap-modified MBs were washed three times with hybridization buffer and resuspended in 200 μL of the same buffer solution. After that 40 μL of the hybridization solution containing Signal probe (Sp) was added into the Ap-modified MBs to hybridize for 1 h at 37 °C. Finally, the Ap–Sp modified MBs were washed three times with sodium citrate buffer and resuspended in 200 μL of the same buffer solution.

2.3. Preparation of the fluorescent aptasensor for OTA detection

Different concentrations of OTA solution were added into the Ap–Sp modified MBs *solution*. After magnetic separation by a neodymium magnet placed under the centrifuge tube, 60 μL of the supernatant liquid was mixed with 10 μL 1 mM $AgNO_3$ and 80 μL of sodium citrate buffer (10 mM, pH 7.0) by vortex. Then the mixtures were kept at room temperature in dark. After 10 min, 100 μL of 200 μM freshly prepared $NaBH_4$ was added with vortex, and then *was allowed to react* at 45 °C for 5 min. The resulting solutions were transferred to a spectro fluorometer cuvette by a transferpettor. Finally, the photographs of the mixture were taken with a digital camera, and the UV–vis absorption spectra were measured in the wavelength range from 500 nm to 700 nm, while the fluorescence spectra were recorded in the wavelength range from 600 nm to 750 nm with the excitation of 574 nm at room temperature.

2.4. CD measurements of Ap-OTA G-quadruplex

The CD spectra of Ap–Sp duplex solution before and after the addition of OTA were all collected with the JASCO spectropolarimeter. The optical chamber (1 cm path length, 500 μL volume) was deoxygenated with dry purified nitrogen (99.99%) before use and the nitrogen atmosphere was maintained during experiments. Three scans (50 nm/min) from 220 nm to 400 nm at 0.1 nm intervals were accumulated and averaged. The background of the buffer solution was subtracted from the CD data.

2.5. Pretreatment of wheat samples

For determination of OTA in wheat, the wheat samples obtained from local agricultural product markets were treated by the official method (National Standards of the People's Republic of China GBT 23502-2009). First, the samples were ground by a high-speed disintegrator. Second, as-prepared sample was passed through a 1 mm aperture test sieve. Then 2 g of the sample and 0.5 g NaCl were introduced into a 10 mL flask and mixed with the extracting solution (methanol+H_2O, 8+2). Third, the resulting mixture was put into the cup of a homogenizer and extracted for 2 min with stirring at high-speed. *After filtration*, 2.0 mL of the filtrate was put into a 10 mL flask for homogenizing. Subsequently, the resulting solution was further filtered with glass fiber filter paper until the filtrate was clear. Finally, the filtrate was diluted with binding buffer for recovery studies.

3. Results and discussion

3.1. Experimental principle of the aptasensor based on DNA-scaffolded AgNCs and MBs

The detailed principle of our sensor is shown in Fig. 1. As shown in Fig. 1, Ap (colored purple) functionalized with a biotin group at one end was attached to streptavidin-modified magnetic beads. The cytosine rich single-strand Sp (colored black) partly complementary to Ap was added to hybridize with Ap to form an Ap–Sp duplex structure. In the presence of OTA, because the stability of the G-quadruplex is higher than that of Ap–Sp duplexes, Ap can bind with OTA to form G-quadruplex while releasing the single-strand Sp. Through magnetic separation, the released Sp was left in the supernatant liquid. Upon the addition of Ag^+, the Sp could act as a scaffold for the synthesis of fluorescent silver nanoclusters (AgNCs) through the reduction of $NaBH_4$ due to the high affinity of Ag^+ and cytosines of Sp. The resulting Sp-scaffolded AgNCs exhibited excellent spectral and photophysical properties with fluorescence emission at 632 nm upon excitation at 574 nm. However, in the absence of OTA, the Ap–Sp modified MBs were separated by a neodymium magnet placed under the centrifuge tube. Therefore, the supernatant liquid contained no single-strand Sp and could not react with Ag^+ to synthesize AgNCs. Using this green chemical sensing platform, a simple, rapid, ultra-highly sensitive and selective, turn-on fluorescence aptasensor for the detection of OTA has been developed.

3.2. Identification of Ap-OTA G-quadruplex by CD spectrum

It is well known that CD spectroscopy is a very useful tool for the detection and characterization of G-quadruplex (Kuang et al., 2010). Our previous study confirmed by CD spectrum that the conformation of Ap could be changed from a random coil structure to a compact rigid antiparallel G-quadruplex structure upon OTA addition (Zhang et al., 2013). In order to study the sensing process of the present aptasensor, the CD spectrum of Ap–Sp duplex solution before and after the addition of OTA was recorded. As shown in Fig. 2, before the addition of OTA, the CD spectrum of Ap–Sp duplex gave a clear CD signal with a positive peak at 264 corresponding to base stacking and one negative peak at around 241 nm corresponding to helicity, indicating a definite two-helical structure (Fig. 2, line a) (Zhang et al., 2002). After the addition of OTA, a dramatic change was observed in the CD spectrum (Fig. 2, line b). A positive peak at 295 nm corresponding to antiparallel G-quadruplex (Balagurumoorthy and Brahmachari, 1994) appeared and the band near 265 nm obviously decreased in the meantime. All above CD results confirmed that the OTA possessed the ability to induce the formation of antiparallel G-quadruplexes structure, indeed corresponding with our expectations.

3.3. Fluorescence and UV–vis measurements of Sp-scaffolded AgNCs

As shown in Fig. 3A, synthesized Sp–AgNCs produce fluorescence emission at 632 nm upon the excitation at 574 nm. At the same time, the stability of the maximum fluorescence emission of

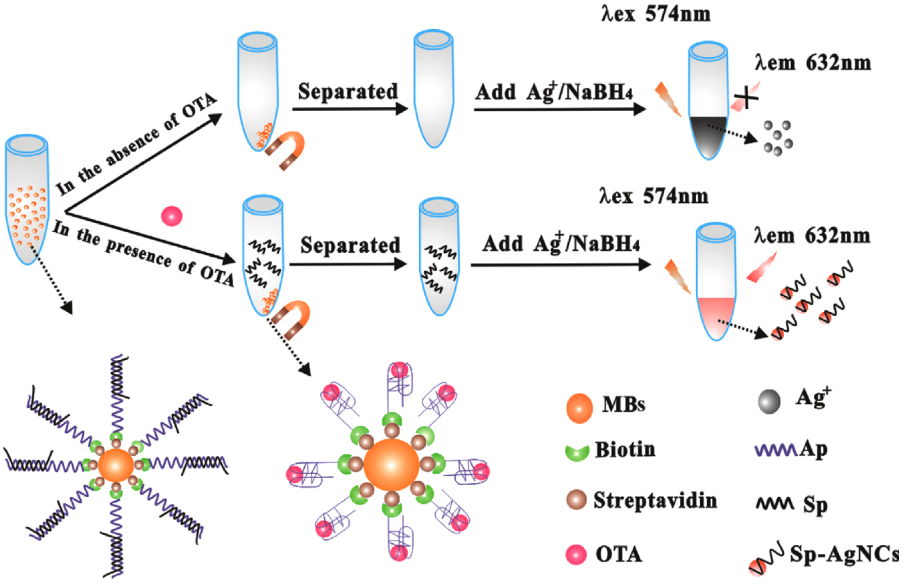

Fig. 1. The principle of the aptasensor. (For interpretation of the references to color in this figure, the reader is referred to the web version of this article.)

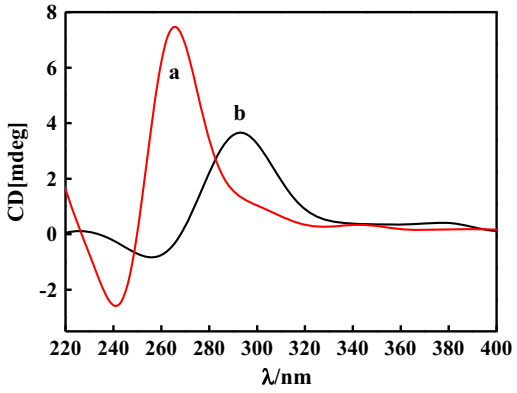

Fig. 2. CD spectra of Ap–Sp duplex before (a) and after (b) the addition of OTA.

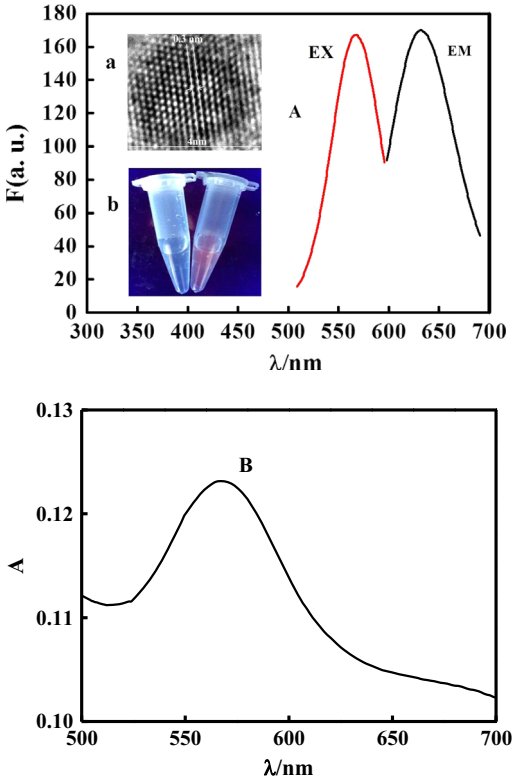

Fig. 3. (A) The maximum excitation and emission spectra of the fluorescent Sp–AgNCs (Ex: 574 nm, Em: 632 nm). Inset: (a) a typical HRTEM image of the Sp–AgNCs (upper image) and (b) a photograph of Sp–AgNCs solution taken under the UV light (below image). (B) The UV/vis spectra of Sp–AgNCs.

Sp–AgNCs when excited at 574 nm was studied as well. The experimental results demonstrated that there was no obvious decrease in the fluorescence intensity at room temperature within 3 h, and only a decrease less than 4.2% after 6 h. Moreover, only less than 3.5% fluorescent decrease was observed with a luminescent spectrometer for even ten consecutive scans. All above results indicate that the Sp–AgNCs have excellent photostability. Furthermore, the HRTEM image of the Sp–AgNCs shows a uniform, monodispersed, well-resolved interference fringe spacing (ca. 0.30 nm), which demonstrate the highly crystalline structure of the Sp–AgNCs (Fig. 3A, a), and the aqueous solution of the Sp–AgNCs shows red luminescence under excitation with an ultraviolet analyzer (Fig. 3A, b). In addition, the spectral properties of Sp–AgNCs were also characterized by UV–vis absorption spectroscopy. Fig. 3B shows a characteristic absorption peak of Sp–AgNCs with a maximum wavelength at 565 nm, which is consistent with those AgNCs templated by oligonucleotide in previous reports (Guo et al., 2013). In a word, DNA–AgNCs have predominant optical characteristics and can be used as a signal indicator for the development of sensitive and effective AgNCs-based OTA biosensors.

3.4. Optimization of experimental conditions

Experimental variables including temperature and time of the hybridization reaction, incubation time for Ap binding, the concentrations of Ag^+ and $NaBH_4$, and the temperature for the synthesis of fluorescent DNA–AgNCs were first optimized (see Fig. S1 in the support information). The maximum fluorescence intensity was observed under the optimal conditions as below: 37 °C and 60 min were used as the optimum temperature and the time of the hybridization reaction, respectively. 1 min was chosen as the incubation time for the Ap binding. 45 °C, 100 μM Ag^+ and 200 μM $NaBH_4$ were used for the synthesis of DNA–AgNCs. Then the effect of other experimental variables such as type and pH of the buffer were also examined in detail. The results showed that the optimum conditions were the sodium citrate buffer (10 mM) and 7.0, correspondingly.

3.5. Sensitivity of the aptasensor

The sensitivity of the proposed aptasensor for accurate quantification of OTA was investigated by varying the OTA concentration under the optimized assay conditions. Due to the fact that the OTA prefer to form the G-quadruplex, the Sp can be released to act as a scaffold for the synthesis of fluorescent AgNCs with Ag^+. As expected, the addition of an increasing amount of OTA resulted in a dynamic increase of fluorescence emission intensity at 632 nm (Fig. 4). A linear relationship between the fluorescence intensity (F) and the concentration of OTA (C) was plotted (the inset of Fig. 4) in the range of 0.01–0.30 ng/mL. The calibration equation obtained from this curve was $F=464.9C+11.44$ with a correlation coefficient of 0.9918. The calculated limit of detection (LOD) was 2 pg/mL with a signal-to-noise ratio of 3. The repeatability of the aptasensor was also evaluated by measuring the fluorescence intensity of the same sample (0.1 ng/mL OTA) five times, and a relative standard deviation (RSD) of 1.5% was obtained, showing a good repeatability of the measurements.

In order to further confirm that the higher sensitivity of the proposed aptasensor was partially ascribed to the AgNCs, an analogic labeled fluorescent aptasensor without the AgNCs was designed for OTA detection. As illustrated in Fig. 5B, an Ap hybridized with a partly complementary single-strand signal

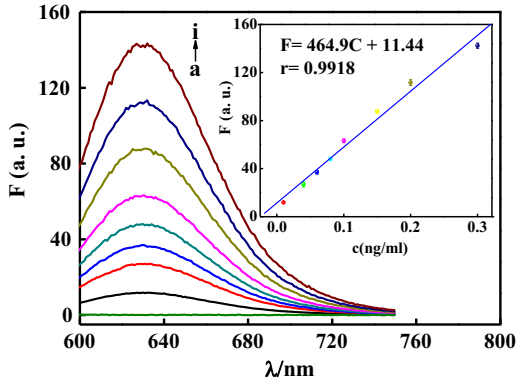

Fig. 4. Fluorescence spectra of the aptasensor with different concentrations of OTA (from a to i): 0.00, 0.01, 0.04,0.06, 0.08,0.10, 0.15, 0.20, and 0.30 ng/mL. (Inset) A calibration curve demonstrating peak fluorescence intensity versus OTA concentration.

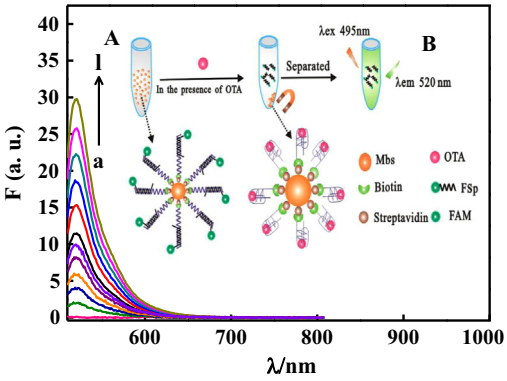

Fig. 5. (A) Fluorescence spectra of different concentrations of OTA (from a to h): 0, 1, 10, 20, 30, 40, 50, 60, 70, 80, 90, and 100 ng/mL. (B) Schematic illustration of an analogic fluorescent aptasensor with label strategy for OTA detection.

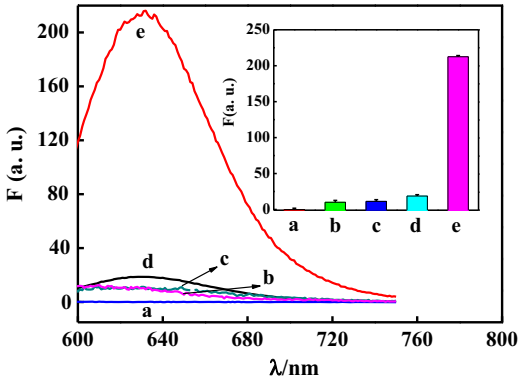

Fig. 6. Selectivity of the aptasensor toward OTA against other mycotoxins at the same concentrations (1 ng/mL). Blank (a), AFB1 (b), FB (c), OTB (d), and OTA (e). (Inset) The histogram of selectivity. Each data point represents the average value of three independent experiments with error bars indicated.

probe (labeled with a fluorophore (FAM) at the 3' end, FSp) to form an Ap–FSp duplex. Upon the addition of OTA, it could bind with Ap to form OTA-Ap G-quadruplexes coupling with a structure switching, resulting in the release of the FSp in the meantime. Through magnetic separation, the FSp was left in the supernatant liquid. Owing to the photophysical properties of FAM, the solution displayed fluorescence emission at 520 nm upon excitation at 495 nm. As shown in Fig. 5A, the fluorescence intensity enhancement increased linearly with increase of OTA concentration in the range from 1 to 100 ng/mL and the LOD was calculated to be 0.5 ng/mL, which was consistent with the results obtained in the previous report (Chen et al., 2012). Compared with the above method, our proposed aptasensor has higher sensitivity due to the high quantum yield and the photostability of AgNCs. At the same time, the aptasensor, containing no fluorescent labeling and purification process, is inexpensive and fast. Furthermore, compared with the previous OTA sensors, such as colorimetric (Yang et al., 2011), chromatographic (Zhang et al., 2009), and electrochemical (Radi et al., 2009) detection methods, this aptasensor also exhibits higher sensitivity. In addition, owing to the fact that the photoluminescence emission band of DNA–AgNCs can be fine-tuned just by changing the sequence of used DNA, the proposed aptasensor can detect multiple mycotoxins simultaneously.

3.6. Selectivity of the aptasensor

A superordinary assay for practical implementation of OTA detection not only ought to be sensitive to different concentrations of OTA, but also must be specific. In order to evaluate the selectivity of the present aptasensor, we compared the change of fluorescence intensity induced by the same concentrations of three other mycotoxins, including OTB, AFB1, and FB. As shown in Fig. 6, the aptasensor exhibited different response signals to the above mycotoxins. The sensing results of the AFB1 and FB were almost neglectable (Fig. 6, curves b and c, respectively). Moreover, the fluorescence intensity of OTB (Fig. 6, curve d) was less than 8.5% of that of OTA (Fig. 6, curve e) although OTB is a structural analog of OTA. Compared with the monoclonal antibody or polyclonal antibodies based methods, the difference in affinity between OTA and OTB of our aptamer-based biosensor is far greater (Cruz-Aguado and Penner, 2008a and 2008b). Thus, the developed aptasensor presents an ultra-high selectivity, which is sufficient for practical applications.

3.7. Determination of OTA in wheat samples

With decrease of OTA restrictive levels in wheat defined by EU and other developed countries, the development of more robust methods for the determination of OTA is urgently requested. In order to evaluate the feasibility and reliability, the aptasensor was used for determining the recoveries by spiking three different concentrations of OTA into the real wheat samples. As shown in Table S2 (see details from the support information), the recoveries were between 93% and 108% ($n=5$), implying that the proposed aptasensor could therefore be applied to the quantitative determination of OTA in agricultural commodities samples.

4. Conclusions

In this work, we develop an ultra-highly sensitive and selective fluorescent aptasensor based on fluorescent DNA-scaffolded AgNCs and MBs for OTA determination as low as picogram sensitivity and demonstrate its feasibility in the application of detection of OTA in wheat. Benefiting from the extraordinary fluorescence properties of AgNCs including high quantum yields, high stability, good biocompatibility and nontoxicity, the proposed ultra-sensitive aptasensor is a brand-new but promising candidate for OTA detection. More importantly, due to the fact that the photoluminescence emission band of DNA–AgNCs can be fine-tuned just by changing the used DNA sequence, combined and simultaneous detection of multiple mycotoxins can be potentially realized by rational designing corresponding aptamer probe and signal probe according to various mycotoxins. In addition, owing to the use of MBs, the separation and the detection processes of the proposed sensor can be achieved simultaneously, and the cleaning and reusing procedures are simplified by means of a neodymium magnet placed under the centrifuge tube. In summary, due to its ultra-highly sensitivity and selectivity, being fast and inexpensive, the proposed aptasensor may represent a promising way for combined detection of multi-mycotoxin, especially for the field monitoring and the large-scale screening.

Acknowledgments

The authors gratefully acknowledge the financial support of the National Basic Research Program of China (973 Program, 2013CB127802), the financial support of National Natural Science Foundation of China (21375017, 21105012, and 21205015), National Science Foundation for Distinguished Young Scholars of Fujian Province (2013J06003), Program for New Century Excellent Talents in University of China (NCET-10-0010), the *Key Project of Fujian Science and Technology (2013Y0045)*, *Agricultural Five New Projects of Fujian* Development and Reform Commission, National

Science Foundation of Fujian Province (2011J01028), Program for Fujian University Outstanding Youth Scientific Research (JA11105 and JA10295), Program for New Century Excellent Talents of Colleges and Universities in Fujian Province (JA13130), the Youth Foundation of Fujian Health Department (2010126) and the Foundation of Medical Innovation of Fujian Health Department (2011-CX-22), The Foundation of Fuzhou Science and Technology Bureau (2012-S-148).

Appendix A. Supporting information

Supplementary data associated with this article can be found in the online version at http://dx.doi.org/10.1016/j.bios.2014.02.001.

References

Chen, J., Fang, Z., Liu, J., Zeng, L., 2012. Food Control 25, 555–560.
Clarke, J.R., Marquardt, R.R., Oosterveld, A., Frohlich, A.A., 1993. J. Agric. Food Chem. 41, 1784–1789.
Cruz-Aguado, J.A., Penner, G., 2008a. Anal. Chem. 80, 8853–8855.
Cruz-Aguado, J.A., Penner, G.J., 2008b. Agric. Food Chem. 56, 10456–10461.
Diez, I., Ras, R.H.A., 2011. Nanoscale 3, 1963–1970.
Guo, W.W., Yuan, J.P., Dong, Q.Z., Wang, E.K., 2010. J. Am. Chem. Soc. 132, 932–934.
Guo, X.Q., Deng, L., Wang, J.X., 2013. RSC Adv. 3, 401–407.
Huang, Z.Z., Pu, F., Hu, D., Wang, C.Y., Ren, J.S., Qu, X.G., 2011. Chemistry 17, 3774–3780.
Hun, X., Liu, F., Mei, Z.H., Ma, L.F., Wang, Z.P., Luo, X.L., 2013. Biosens. Bioelectron. 39, 145–151.
Kuang, H., Chen, W., Xu, D.H., Xu, L.G., Zhu, Y.Y., Liu, L.Q., Chu, H.Q., Lan, G.Y., Huang, C.C., Chang, H.T., 2010. Chem. Commun. 46, 1257–1259.
Lan, G.Y., Huang, C.C., Chang, H.T., 2010. Chem. Commun. 46, 1257–1259.
Liu, Y.Q., Zhang, M., Yin, B.C., Ye, B.C., 2012. Anal. Chem. 84, 5165–5169.
Ma, K., Cui, Q.H., Liu, G.Y., Wu, F., Xu, S.J., Shao, Y., 2011. Nanotechnology 22, 305502.
Ma, W., Yin, H.H., Xu, L.G., Xu, Z., Kuang, H., Wang, L.B., Xu, C.L., 2013. Biosens. Bioelectron. 42, 545–549.
O'Brien, E., Dietrich, D.R., 2005. Crit. Rev. Toxicol. 35, 33–60.
Radi, A.E., Munoz-Berbel, X., Cortina-Puig, M., Marty, J.L., 2009. Electrochim. Acta 54, 2180–2184.
Richards, C.I., Choi, S., Hsiang, J.C., Antoku, Y., Vosch, T., Bongiorno, A., Tzeng, Y.L., Dickson, R.M., 2008. J. Am. Chem. Soc. 130, 5038–5039.
Richards, C.I., Hsiang, J.C., Senapati, D., Patel, S., Yu, J., Vosch, T., Dickson, R.M., 2009. J. Am. Chem. Soc. 131, 4619–4621.
Ritchie, C.M., Johnsen, K.R., Kiser, J.R., Antoku, Y., Dickson, R.M., Petty, J.T., 2007. J. Phys. Chem. C 111, 175–181.
Sheng, L.F., Ren, J.T., Miao, Y.Q., Wang, J.H., Wang, E.K., 2011. Biosens. Bioelectron. 26, 3494–3499.
Tong, P., Zhao, W.W., Zhang, L., Xu, J.J., Chen, H.Y., 2012. Biosens. Bioelectron. 33, 146–151.
Yang, C., Wang, Y., Marty, J.L., Yang, X.R., 2011. Biosens. Bioelectron. 26, 2724–2727.
Yang, S.W., Vosch, T., 2011. Anal. Chem. 83, 6935–6939.
Yin, J.J., He, X.X., Wang, K.M., Qing, Z.H., Wu, X., Shi, H., Yang, X.H., 2012. Nanoscale 4, 110–112.
Zhang, J., Zhang, X., Yang, G.D., Chen, J.H., Wang, S.H., 2013. Biosens. Bioelectron. 15, 704–709.
Zhang, Z., Huang, W., Tang, J., Wang, E., Dong, S., 2002. Biophys. Chem. 97, 7–16.
Balagurumoorthy, P., Brahmachari, S.K., 1994. J. Biol. Chem. 269, 21858–21869.
Zhang, X., Cudjoe, E., Vuckovic, D., Pawliszyn, J., 2009. J. Chromatogr. A 1216, 7505–7509.